



# Numerical solution of the phase change problem around a horizontal cylinder in the presence of natural convection in the melt region

Kamal A.R. Ismail \*, Maria das Graças E. da Silva

*Department of Thermal and Fluid Engineering, Faculty of Mechanical Engineering, State University of Campinas, P.O. Box 6122, 13083-970 Campinas, SP, Brazil*

Received 24 May 2002; received in revised form 7 November 2002

## Abstract

This paper deals with the numerical study of melting of phase change material around a horizontal circular cylinder in the presence of the natural convection in the melt phase. A two dimensional unsteady mathematical model has been formulated in terms of primitive variables and a coordinate transformation technique has been used to fix the moving front. The finite volume approach was used to discretize the system of governing equations, boundary and initial conditions and obtain a system of linear algebraic equations. In the numerical solution an implicit scheme was used for the momentum and energy equations and an explicit scheme for the energy balance at the interface. The numerical predictions were compared with available results to establish the validity of the model and the numerical approach.

© 2003 Published by Elsevier Science Ltd.

*Keywords:* Fusion of PCM; Phase change; Horizontal cylinder; Natural convection

## 1. Introduction

Basically there are two methods for formulating the problem of heat transfer with phase change. The first method uses the temperature as a dependent variable while the second uses the enthalpy as a dependent variable in the energy equation. In the models based upon the temperature, the energy equation is written separately for each phase and the coupling between the two equations is done through the energy balance at the solid–liquid interface. In this type of formulation it is necessary to know explicitly the position of the interface in order to determine the temperature. Having a moving interface not known before hand complicates the problem and its solution. One of the methods to solve the problem is to immobilize the interface as done by Landau [1], Duda et al. [2], Saitoh [3] and Sparrow et al. [4].

A second method is to use the enthalpy as a dependent variable and hence write a single energy equation for the whole domain, liquid and solid. This method has the advantage of not requiring to determine the interface position in order to solve the energy equation. Comparative studies of the two methods can be found in Furzerland [5], Viswanath and Jaluria [6]. A pioneer study realized by Sparrow et al. [7] of fusion around a vertical cylinder showed that natural convection could not be ignored in the analysis of fusion problems. Later Yao and Chen [8] determined an approximate solution for the fusion problem around a horizontal constant temperature cylinder by using the perturbation technique. They studied the effect of natural convection on the fusion process and concluded that it depends strongly on the Rayleigh number. Yao and Cherney [9] resolved the case of fusion around a horizontal constant temperature cylinder by using the integral method. Rieger et al. [10] solved numerically the problem of fusion around a horizontal cylinder under the conditions of constant wall temperature and constant heat flux over the cylinder wall. They included natural convection in

\* Corresponding author. Tel.: +55-19-3788-3376; fax: +55-19-3788-3722.

E-mail address: [kamal@fem.unicamp.br](mailto:kamal@fem.unicamp.br) (K.A.R. Ismail).

### Nomenclature

$c_{pL}$	liquid specific heat, $\text{J kg}^{-1} \text{C}^{-1}$
$g$	gravity acceleration, $\text{m s}^{-2}$
$k_L$	liquid thermal conductivity, $\text{W m}^{-1} \text{C}^{-1}$
$L$	latent heat, $\text{J kg}^{-1}$
$P$	dimensionless pressure
$Pr$	Prandtl number ( $= \nu/\alpha$ )
$r_o$	cylinder radius, m
$r$	radial coordinate, m
$r_L$	interface position, m
$R$	dimensionless radial coordinate
$R_L$	dimensional interface position
$Ra$	Rayleigh number based on temperature ( $= g\beta(T_o - T_m)r_o^3/\nu\alpha$ )
$Ra_q$	Rayleigh number based on heat flux ( $= g\beta q r_o^4/\nu\alpha k$ )
$Ste$	Stefan number based on temperature ( $= c_p(T_o - T_m)/L$ )
$St_q$	Stefan number based upon heat flux ( $= c_p q r_o/Lk$ )
$t$	time, s
$T$	temperature of the liquid phase, $^{\circ}\text{C}$
$T_{\text{mean}}$	bulk temperature, $^{\circ}\text{C}$
$V_{\theta}$	dimensionless velocity component in the tangential direction

$V_R$  dimensionless velocity component in the radial direction

#### Greek symbols

$\alpha_L$	liquid thermal diffusivity, $\text{m}^2 \text{s}^{-1}$
$\beta$	coefficient of thermal expansion, $\text{K}^{-1}$
$\phi$	dimensionless temperature
$\Delta_L$	dimensionless melt thickness
$\eta$	transformed radial coordinate
$\mu_L$	liquid dynamic viscosity, $\text{kg m}^{-1} \text{s}^{-1}$
$\nu_L$	liquid kinematic viscosity, $\text{m}^2 \text{s}^{-1}$
$\theta$	angular coordinate
$\rho_L$	liquid density, $\text{kg m}^{-3}$
$\tau$	dimensionless time
$\bar{A}, A, \Theta, \Omega, \Psi$	auxiliary variables
$\forall$	volume

#### Superscript

\* dimensionless variables

#### Subscripts

L	liquid
m	phase change
o	surface of the cylinder
R	radial direction
$\theta$	angular direction

the liquid phase and used body fitted coordinate technique to immobilize the fusion front. Prusa and Yao [11,12] analysed numerically the effects of natural convection during the process of fusion around a horizontal cylinder. They used the technique of coordinate transformation to fix the irregular moving interface and finite difference approach to solve the problem numerically. Additional experimental results and comparisons were realized by Hermann et al. [13] and Ho and Chen [14].

The problem of melting around a circular cylinder as available in the literature, specifically, Yao and Chen [8], Yao and Cherney [9], Rieger et al. [10] and Prusa and Yao [11,12] is formulated based on the stream function and vorticity method, except the work of Sparrow et al. [7] which is based upon primitive variables formulation. In Sparrow et al. [7] work, the terms resulting from the transformation of coordinates were eliminated in order to simplify the solution of the problem. The contribution of the present work is that the proposed formulation is based upon primitive variables, transformation of coordinates while keeping all the resulting terms and finally that the solution involved the control volume approach.

The present paper deals with the numerical study of melting of phase change material (PCM) around a horizontal circular cylinder in the presence of natural convection in the melt phase. A two-dimensional non-steady mathematical model has been formulated in

terms of the primitive variables and a coordinate transformation has been used to fix the moving interface. The finite volume approach was used to discretize the system of governing equations and the associated boundary and initial conditions to obtain a system of linear algebraic equations. The numerical code was optimized and the numerical predictions were compared with available numerical results to establish the validity of the model and the adopted numerical approach.

## 2. Mathematical model

The physical problem is shown in Fig. 1. The horizontal cylinder of radius  $r_o$  is immersed in an infinite solid PCM. At the instant  $t = 0$ , the PCM is at the phase change temperature  $T_m$ . When the cylinder surface temperature is at  $T_o > T_m$ , the melting process starts. Two melting cases will be treated here. The first when the surface temperature of the cylinder  $T_o > T_m$  while the other of specified heat flux  $q$ . The general simplifications considered in this study include transient formulation and two-dimensional Newtonian incompressible fluid where the natural convection effects are considered. The thermophysical properties of the PCM are assumed constant except the density.

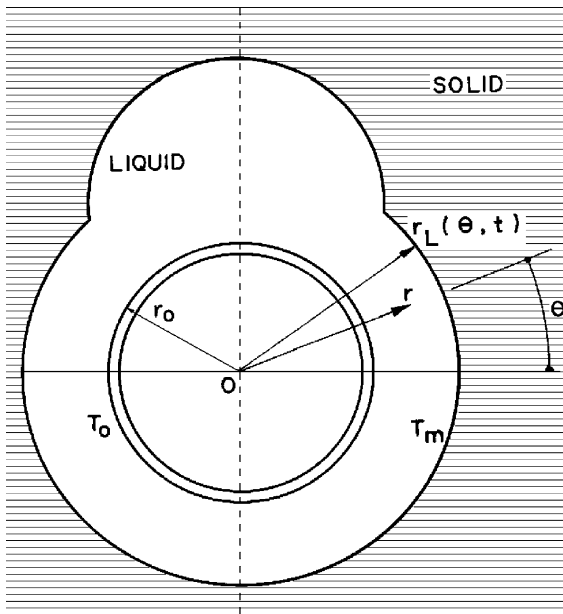


Fig. 1. Layout of the physical problem.

The basic equations can be written as

Energy conservation equation

$$\frac{\partial T}{\partial t} + \frac{1}{r} \frac{\partial(rV_R^*T)}{\partial r} + \frac{1}{r} \frac{\partial(V_\theta^*T)}{\partial \theta} = \alpha_L \left( \frac{1}{r} \frac{\partial}{\partial r} \left( r \frac{\partial T}{\partial r} \right) + \frac{1}{r^2} \frac{\partial^2 T}{\partial \theta^2} \right) \quad (1)$$

Conservation of mass

$$\frac{1}{r} \frac{\partial(rV_R^*)}{\partial r} + \frac{1}{r} \frac{\partial V_\theta^*}{\partial \theta} = 0 \quad (2)$$

Equation of motion in the tangential direction

$$\frac{\partial V_\theta^*}{\partial t} + \frac{1}{r} \frac{\partial(rV_R^*V_\theta^*)}{\partial r} + \frac{1}{r} \frac{\partial(V_\theta^*)^2}{\partial \theta} + \frac{V_R^*V_\theta^*}{r} = -\frac{1}{\rho_L} \frac{1}{r} \frac{\partial P^*}{\partial \theta} + \bar{A} \cos \theta + v_L \left( \frac{1}{r} \frac{\partial}{\partial r} \left( r \frac{\partial V_\theta^*}{\partial r} \right) + \frac{1}{r^2} \frac{\partial^2 V_\theta^*}{\partial \theta^2} - \frac{V_\theta^*}{r^2} + \frac{2}{r^2} \frac{\partial V_R^*}{\partial \theta} \right) \quad (3)$$

Equation of motion in the radial direction

$$\frac{\partial V_R^*}{\partial t} + \frac{1}{r} \frac{\partial r(V_R^*)^2}{\partial r} + \frac{1}{r} \frac{\partial(V_\theta^*V_R^*)}{\partial \theta} - \frac{(V_\theta^*)^2}{r} = -\frac{1}{\rho_L} \frac{\partial P^*}{\partial r} + \bar{A} \sin \theta + v_L \left( \frac{1}{r} \frac{\partial}{\partial r} \left( r \frac{\partial V_R^*}{\partial r} \right) + \frac{1}{r^2} \frac{\partial^2 V_R^*}{\partial \theta^2} - \frac{V_R^*}{r^2} - \frac{2}{r^2} \frac{\partial V_\theta^*}{\partial \theta} \right) \quad (4)$$

where the term  $\bar{A}$  is given by  $\bar{A} = \beta g(T - T_m)$ .

The initial and boundary conditions for Eqs. (1)–(4) are

$$T = T_m; \quad V_\theta^* = 0; \quad V_R^* = 0 \quad \text{at } t = 0 \quad (5)$$

$$T = T_o; \quad V_\theta^* = 0; \quad V_R^* = 0 \quad \text{at } r = r_o, \quad t > 0 \quad (6)$$

$$\frac{\partial T}{\partial \theta} = 0; \quad V_\theta^* = 0; \quad \frac{\partial V_R^*}{\partial \theta} = 0 \quad \text{at } \theta = \pm 90, \quad t > 0 \quad (7)$$

Eq. (6) is used for the case of constant wall temperature. The case of constant wall heat flux is given by

$$-k_L \frac{\partial T}{\partial r} = q; \quad V_\theta^* = 0; \quad V_R^* = 0 \quad \text{at } r = r_o, \quad t > 0 \quad (8)$$

The boundary conditions at the solid–liquid interface are given by

$$T = T_m; \quad V_\theta^* = 0; \quad V_R^* = 0 \quad \text{at } r = r_L, \quad t > 0 \quad (9)$$

$$\left[ 1 + \left( \frac{1}{r_L} \frac{\partial r_L}{\partial \theta} \right)^2 \right] \left( -k_L \frac{\partial T}{\partial r} \right) = \rho_L L \frac{\partial r_L}{\partial t} \quad \text{at } r = r_L, \quad t > 0 \quad (10)$$

The problem of phase change in the presence of natural convection is extremely difficult to handle. To reduce these difficulties, the front immobilisation technique is used where the coordinates  $r$  and  $\theta$  are transformed to  $\eta$  and  $\theta$  where

$$\eta = \frac{r - r_o}{r_L - r_o}$$

And the new domain is defined by  $0 \leq \eta \leq 1$  and  $-90 \leq \theta \leq 90$ .

In order to facilitate the numerical calculations the new coordinate system and also new dimensionless variables are adopted. These variables are

$$R = \frac{r}{r_o} \quad \text{and} \quad R_L = \frac{r_L}{r_o}$$

$$\Delta_L = R_L - 1 \quad \text{and} \quad \eta = \frac{R - 1}{\Delta_L}$$

$$\tau = \frac{\alpha_L t}{r_o^2} Ste \quad \text{and} \quad \phi = \frac{T - T_m}{T_o - T_m},$$

for the case of constant surface temperature;

$$\tau = \frac{\alpha_L t}{r_o^2} St_q \quad \text{and} \quad \phi = \frac{T - T_m}{(qr_o/k_L)},$$

for the case of constant wall heat flux;

$$V_\theta = \frac{V_\theta^* r_o}{\alpha_L}; \quad V_R = \frac{V_R^* r_o}{\alpha_L}; \quad P = \frac{P^*}{\rho_L (\alpha_L / r_o)^2};$$

$$Ste = \frac{C_{pL}(T_o - T_m)}{L}; \quad St_q = \frac{C_{pL}qr_o}{Lk_L}$$

Substituting the new variables in Eqs. (1)–(10), these equations are written as below Equation of energy conservation

$$\begin{aligned}
 Ste \frac{\partial \phi}{\partial \tau} + \frac{1}{R\Delta_L} \frac{\partial}{\partial \eta} (RV_R \phi) + \frac{1}{R} \frac{\partial (V_\theta \phi)}{\partial \theta} \\
 = \frac{1}{R\Delta_L} \frac{\partial}{\partial \eta} \left( \frac{R}{\Delta_L} \frac{\partial \phi}{\partial \eta} \right) + \frac{1}{R^2} \frac{\partial^2 \phi}{\partial \theta^2} + \Omega_{liq}
 \end{aligned} \tag{11}$$

where

$$\begin{aligned}
 \Omega_{liq} = & \frac{\eta Ste}{\Delta_L} \frac{\partial \Delta_L}{\partial \tau} \frac{\partial \phi}{\partial \eta} + \frac{\eta}{R\Delta_L} \frac{\partial \Delta_L}{\partial \theta} \frac{\partial (V_\theta \phi)}{\partial \eta} + \frac{2\eta}{R^2 \Delta_L^2} \left( \frac{\partial \Delta_L}{\partial \theta} \right)^2 \\
 & \times \frac{\partial \phi}{\partial \eta} - \frac{\eta}{R^2 \Delta_L} \frac{\partial^2 \Delta_L}{\partial \theta^2} \frac{\partial \phi}{\partial \eta} - \frac{\eta}{R^2 \Delta_L} \frac{\partial \Delta_L}{\partial \theta} \frac{\partial^2 \phi}{\partial \theta \partial \eta}
 \end{aligned}$$

Equation of mass conservation

$$\frac{1}{R\Delta_L} \frac{\partial}{\partial \eta} (RV_R) + \frac{1}{R} \frac{\partial V_\theta}{\partial \theta} - \Omega_{cm} = 0 \tag{12}$$

where

$$\Omega_{cm} = \frac{\eta}{R\Delta_L} \frac{\partial \Delta_L}{\partial \theta} \frac{\partial V_\theta}{\partial \eta}$$

Equation of motion in the tangential direction

$$\begin{aligned}
 Ste \frac{\partial V_\theta}{\partial \tau} + \frac{1}{R\Delta_L} \frac{\partial}{\partial \eta} (RV_R V_\theta) + \frac{1}{R} \frac{\partial V_\theta^2}{\partial \theta} \\
 = -\frac{1}{R} \frac{\partial P}{\partial \theta} + \frac{1}{R\Delta_L} \frac{\partial}{\partial \eta} \left( \frac{PrR}{\Delta_L} \frac{\partial V_\theta}{\partial \eta} \right) + \frac{Pr}{R^2} \frac{\partial^2 V_\theta}{\partial \theta^2} \\
 + \Psi_{ang} + \Omega_{ang}
 \end{aligned} \tag{13}$$

where

$$\Psi_{ang} = PrA \cos \theta - \frac{V_\theta V_R}{R} - \frac{V_\theta Pr}{R^2} + \frac{2Pr}{R^2} \frac{\partial V_R}{\partial \theta}$$

and

$$\begin{aligned}
 \Omega_{ang} = & \frac{\eta}{R\Delta_L} \frac{\partial \Delta_L}{\partial \theta} \frac{\partial P}{\partial \eta} + \frac{\eta Ste}{\Delta_L} \frac{\partial \Delta_L}{\partial \tau} \frac{\partial V_\theta}{\partial \eta} + \frac{\eta}{R\Delta_L} \frac{\partial \Delta_L}{\partial \theta} \frac{\partial V_\theta^2}{\partial \eta} \\
 & + \frac{2\eta Pr}{R^2 \Delta_L^2} \left( \frac{\partial \Delta_L}{\partial \theta} \right)^2 \frac{\partial V_\theta}{\partial \eta} - \frac{\eta Pr}{R^2 \Delta_L} \frac{\partial^2 \Delta_L}{\partial \theta^2} \frac{\partial V_\theta}{\partial \eta} \\
 & - \frac{\eta Pr}{R^2 \Delta_L} \frac{\partial \Delta_L}{\partial \theta} \frac{\partial^2 V_\theta}{\partial \theta \partial \eta} - \frac{2\eta Pr}{R^2 \Delta_L^2} \frac{\partial \Delta_L}{\partial \theta} \frac{\partial V_R}{\partial \eta}
 \end{aligned}$$

Equation of motion in the radial direction

$$\begin{aligned}
 Ste \frac{\partial V_R}{\partial \tau} + \frac{1}{R\Delta_L} \frac{\partial}{\partial \eta} (RV_R^2) + \frac{1}{R} \frac{\partial (V_R V_\theta)}{\partial \theta} \\
 = -\frac{1}{\Delta_L} \frac{\partial P}{\partial \eta} + \frac{1}{R\Delta_L} \frac{\partial}{\partial \eta} \left( \frac{PrR}{\Delta_L} \frac{\partial V_R}{\partial \eta} \right) + \frac{Pr}{R^2} \frac{\partial^2 V_R}{\partial \theta^2} \\
 + \Omega_{rad} + \Psi_{rad}
 \end{aligned} \tag{14}$$

where

$$\Psi_{rad} = PrA \sin \theta + \frac{V_\theta^2}{R} - \frac{V_R Pr}{R^2} - \frac{2Pr}{R^2} \frac{\partial V_\theta}{\partial \theta}$$

and

$$\begin{aligned}
 \Omega_{rad} = & \frac{\eta}{R\Delta_L} \frac{\partial \Delta_L}{\partial \theta} \frac{\partial (V_\theta V_R)}{\partial \eta} + \frac{\eta Ste}{\Delta_L} \frac{\partial \Delta_L}{\partial \tau} \frac{\partial V_R}{\partial \eta} \\
 & + \frac{2\eta Pr}{R^2 \Delta_L^2} \left( \frac{\partial \Delta_L}{\partial \theta} \right)^2 \frac{\partial V_R}{\partial \eta} - \frac{\eta Pr}{R^2 \Delta_L} \frac{\partial^2 \Delta_L}{\partial \theta^2} \frac{\partial V_R}{\partial \eta} \\
 & - \frac{\eta Pr}{R^2 \Delta_L} \frac{\partial \Delta_L}{\partial \theta} \frac{\partial^2 V_R}{\partial \theta \partial \eta} + \frac{2\eta Pr}{R^2 \Delta_L} \frac{\partial \Delta_L}{\partial \theta} \frac{\partial V_\theta}{\partial \eta}
 \end{aligned}$$

The initial, boundary and interface conditions can be written as

$$\phi = 0; \quad V_\theta = 0; \quad V_R = 0 \quad \text{at } \tau = 0 \tag{15}$$

$$\phi = 1; \quad V_\theta = 0; \quad V_R = 0 \quad \text{at } \eta = 0, \tau > 0 \tag{16}$$

In the case of specified heat flux one can write:

$$-\frac{1}{\Delta_L} \frac{\partial \phi}{\partial \eta} = 1; \quad V_\theta = 0; \quad V_R = 0 \quad \text{at } \eta = 0, \tau > 0 \tag{17}$$

The interface conditions are

$$\phi = 0; \quad V_\theta = 0; \quad V_R = 0 \quad \text{at } \eta = 1, \tau > 0 \tag{18}$$

$$\begin{aligned}
 \left[ 1 + \left( \frac{1}{(\Delta_L + 1)} \frac{\partial \Delta_L}{\partial \theta} \right)^2 \right] \left( -\frac{1}{\Delta_L} \frac{\partial \phi}{\partial \eta} \right) \\
 = \frac{\partial \Delta_L}{\partial \tau} \quad \text{at } \eta = 1, \tau > 0
 \end{aligned} \tag{19}$$

The finite volume approach was used to discretize the system of differential equations and obtain a system of linear algebraic equations. The numerical solution was determined using an implicit scheme for the momentum and energy equations and explicit scheme for the energy balance at the interface. Numerical tests were realized in order to optimize the computational grid. Tests were realized to optimize the grid size along the radial direction using 50 points along the angular direction and sets of radial points of 20, 30, 60 and 70. In another set of tests 30 radial points were used together with angular points of 30, 40, 50 and 70. A grid of 50 angular points and 30 radial points was considered satisfactory considering the precision of the results ( $10^{-3}$ ) and the consumed computational time. The time increments used are related to the Rayleigh and Stefan numbers used and are indicated on the graphs.

### 3. Results and discussion

Prusa and Yao [12] studied numerically the problem of fusion around a horizontal cylinder considering natural convection in the liquid phase. In their study they adopted a constant wall temperature on the surface of the cylinder and formulated the phase change problem by using stream and vorticity functions and coordinate

transformation to fix the moving front. They also used an approximate solution for the start of the phase change process.

In order to validate the model the results of the present numerical results are compared with the results due to Prusa and Yao [12]. As can be seen from Fig. 2 the agreement is very good for the case of constant surface temperature. The influence of natural convection on the melting process is indicated by the non-symmetric melting patterns in the top ( $90^\circ$ ) and bottom ( $-90^\circ$ ) parts of the cylinder caused by the convective currents which become dominant for times above  $\tau = 1.0$ .

In another work by the same authors, Prusa and Yao results [11], they treated the same problem of phase change subjected to constant heat flux over the surface of the cylinder and solved by the same approach as in the previous case. For the set of parameters Rayleigh number = 5000, Stefan number = 0.374 and Prandtl number = 54, they obtained curves for the interface position, temperature distribution over the surface of the cylinder temperature distribution in the radial and tangential directions and Nusselt number at the solid–liquid interface. Their results are used to compare with the results of the present model. Fig. 3 shows the thickness of the melt layer as calculated by both models. The agreement is excellent for the position  $\theta = -90^\circ$  and differs slightly for the position  $\theta = 90^\circ$ . These differences can be attributed to the different numerical methods and mathematical model used and the grid size adopted.

Figs. 4 and 5 show comparisons of the surface temperature over the cylinder for the present model and Prusa and Yao [11]. In Fig. 5, one can observe the transition between the regime of dominant conduction

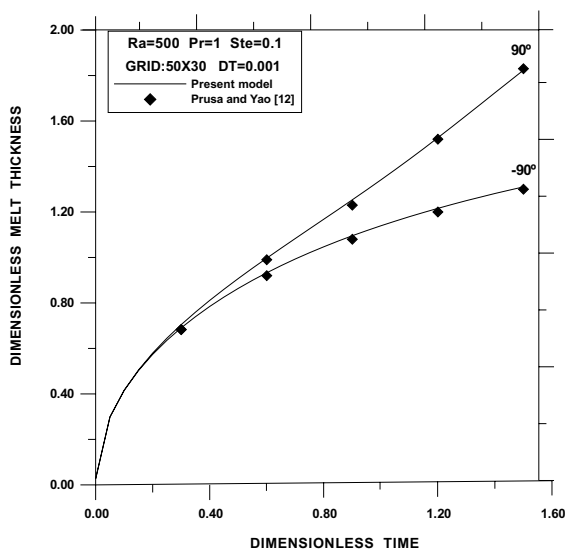


Fig. 2. Comparison of the predicted melt thickness with the results of Prusa and Yao [12].

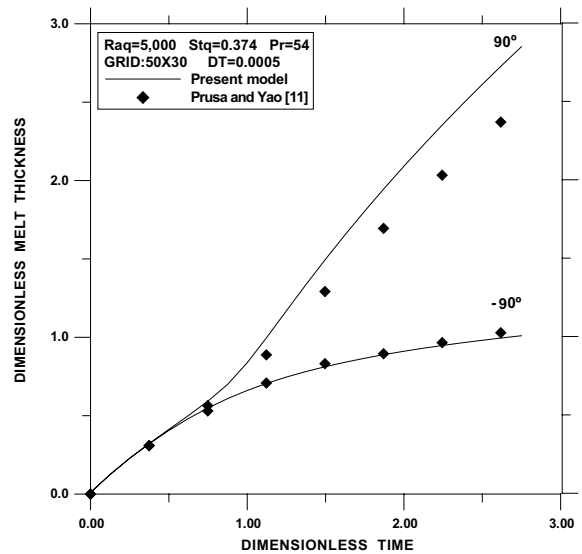


Fig. 3. Comparison of the predicted melt thickness with the results of Prusa and Yao [11].

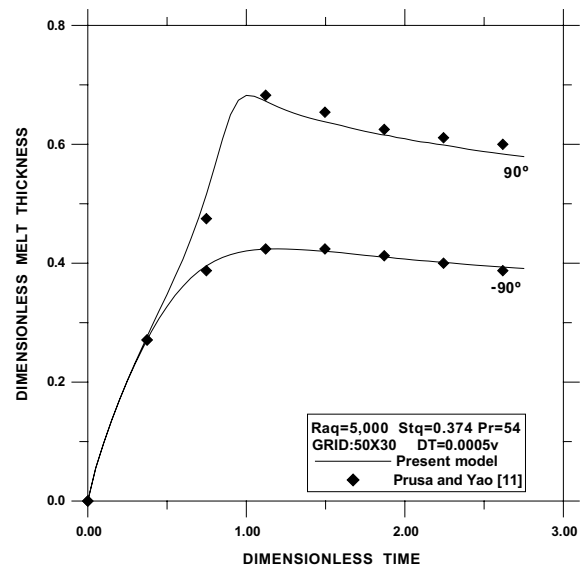


Fig. 4. Comparison of the predicted surface temperature with the results of Prusa and Yao [11].

to the regime of dominant convection. The temperature profiles for the dominant conduction regime ( $\tau = 0.15$  and  $0.374$ ) are horizontal lines. As can be seen in both figures the agreement is very good. Fig. 6 shows another comparison, variation of temperature along lines of constant  $\theta$ , between the present model and Prusa and Yao [11] results indicating good agreement.

Fig. 7 shows the comparative curves for the Nusselt number at the liquid–solid interface. The profile at

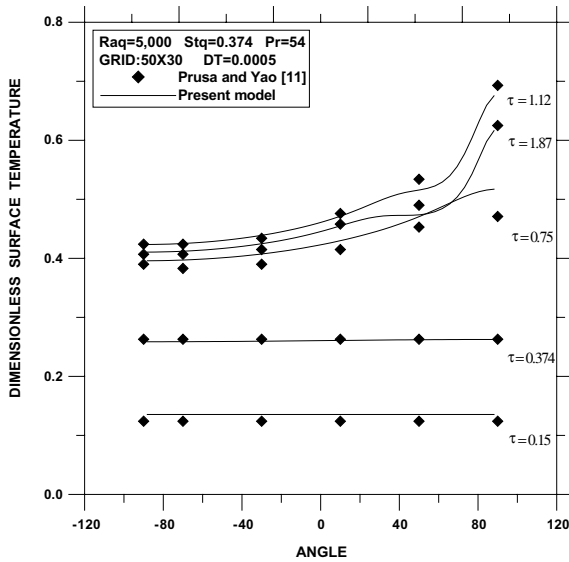


Fig. 5. Comparison of the predicted tangential temperature with the results of Prusa and Yao [11].

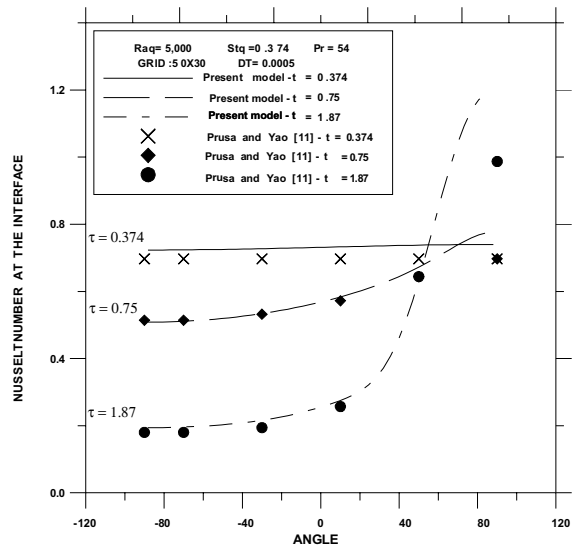


Fig. 7. Comparison of the predicted Nusselt number at the interface with the results of Prusa and Yao [11].

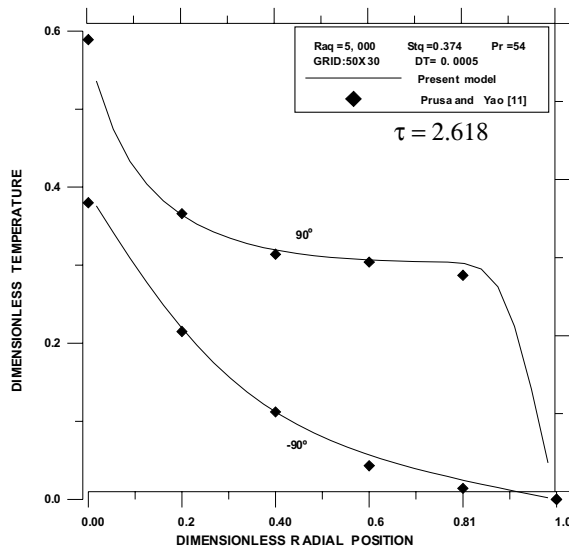


Fig. 6. Comparison of the predicted dimensionless radial temperature with the results of Prusa and Yao [11].

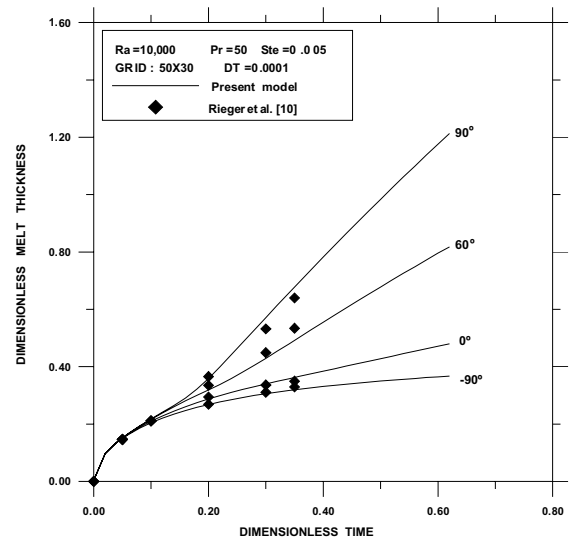


Fig. 8. Comparison of the predicted dimensionless melt thickness with the results of Rieger et al. [10].

$\tau = 0.374$  indicates that the melting process is in the conduction stage, while for  $\tau = 0.75$ , the profile indicates that the melting process reached the transition stage. The results seem to agree relatively well, indicating that the model represents well the case of fusion external to the cylinder for the two cases of constant wall temperature and constant heat flux.

Rieger et al. [10] studied the problem of fusion around a horizontal cylinder under surface constant

temperature. Their model is formulated based upon stream and vorticity functions and body fitted coordinates and finite difference approximation. Their results were compared with the numerical predictions from the present model. Figs. 8 and 9 show the thickness of the melt layer for values of  $Ra = 10^4$  and  $Ra = 37,500$ . As can be noticed the agreement is good. Figs. 10 and 11 show the variation of Nusselt number over the surface of the cylinder for the case of  $Ra = 10^4$  and  $Ra = 37,500$ . It is interesting to observe how transition occurs between the dominant conduction and the dominant convection

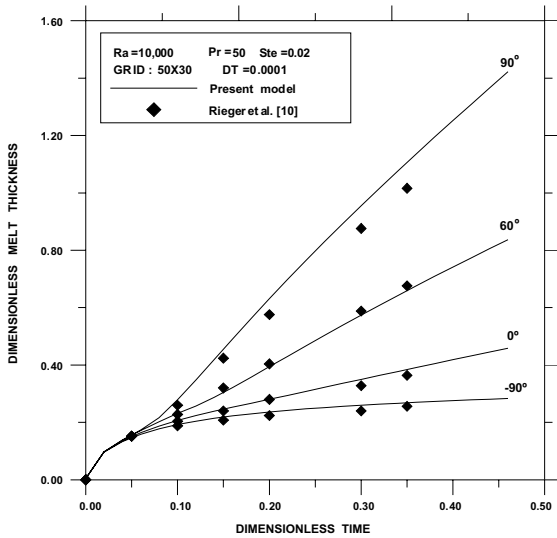


Fig. 9. Comparison of the predicted melt thickness with the results of Rieger et al. [10].

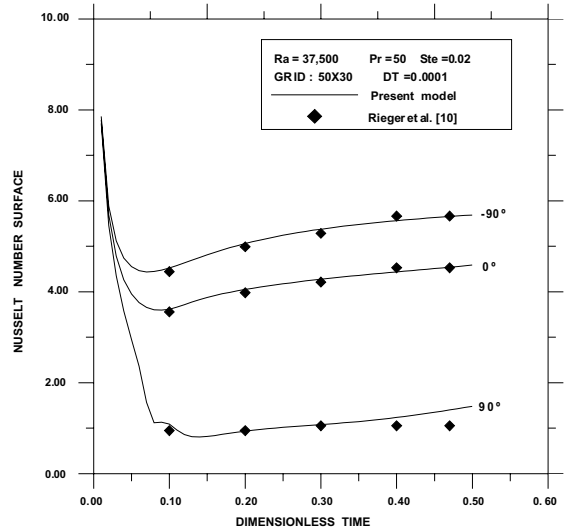


Fig. 11. Comparison of the predicted surface Nusselt number with the results of Rieger et al. [10] for  $Ra = 37,500$ .

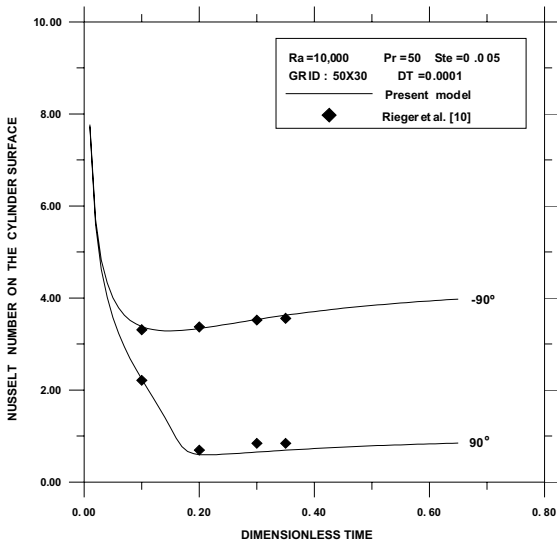


Fig. 10. Comparison of the predicted surface Nusselt number with the results of Rieger et al. [10] for  $Ra = 10^4$ .

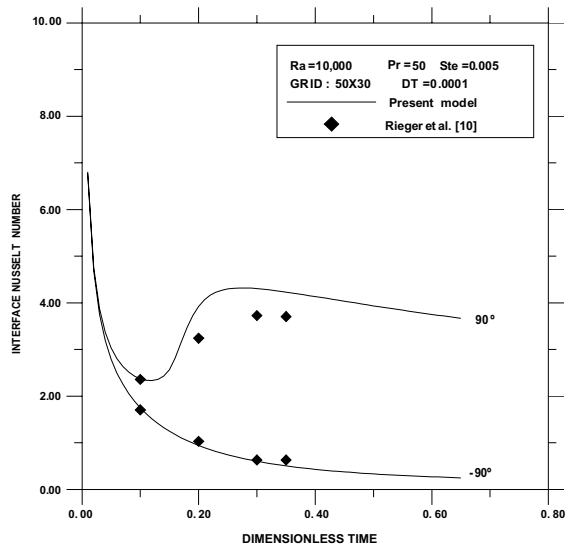


Fig. 12. Comparison of the predicted interface Nusselt number with the results of Rieger et al. [10] for  $Ra = 10^4$ .

regimes as reported by Sparrow et al. [15]. During the dominant conduction process, the curves show a reduction in the Nusselt number. When the dominant convection regime is established the profiles seem to be constant. As can be seen the results agree well indicating that the present model is able to predict precise results. Figs. 12 and 13 show comparisons of Nusselt number at the liquid–solid interface as calculated by Rieger et al. and the present model. The results seem to agree very

well for the case of  $\theta = -90^\circ$  but differs slightly for the position  $\theta = 90^\circ$  although keeping the same tendency. Figs. 14 and 15 show the melt volume as calculated by Rieger et al. and the present model for the two cases of  $Ra = 10^4$  and  $Ra = 37,500$  showing good agreement between the results. One can notice from Figs. 14 and 15, after achieving the dominant convection regime, the melt volume variation with time seems to be linear as reported by Hale and Viskanta [16].

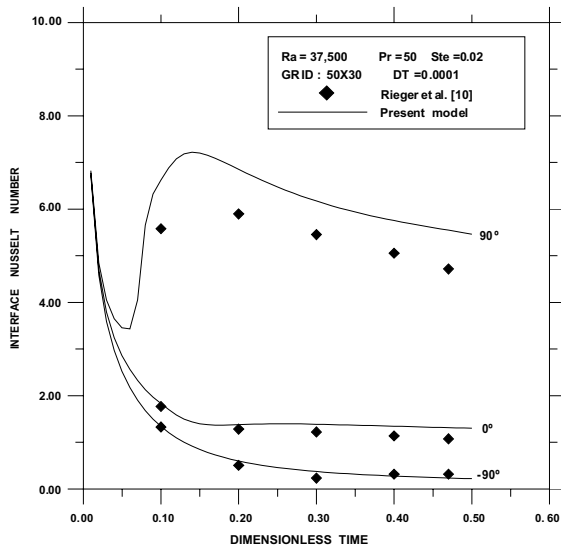


Fig. 13. Comparison of the predicted interface Nusselt number with the results of Rieger et al. [10] for  $Ra = 37,500$ .

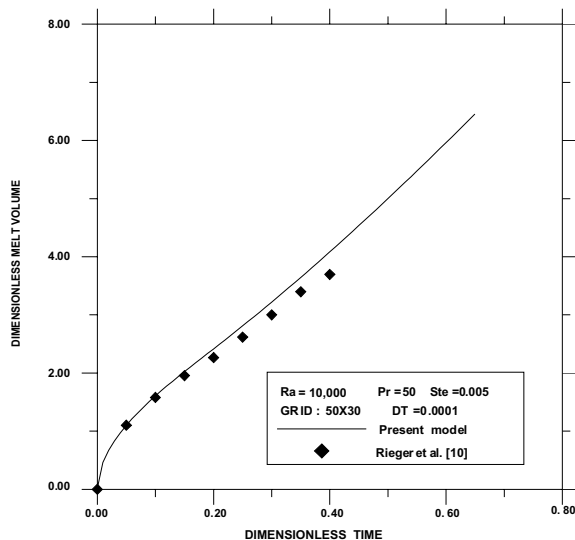


Fig. 14. Comparison of the predicted dimensionless melt volume with the results of Rieger et al. [10] for  $Ra = 10^4$ .

#### 4. Conclusion

A model is proposed in terms of the primitive variables for the fusion around horizontal circular cylinder including natural convection in the melt region. The phase change front was immobilised by using a coordinate transformation and the method of control volumes was used. Two boundary conditions were investigated one of constant wall temperature over the surface of the cylinder and the other of constant heat flux for Rayleigh number as high as 37,500. The predicted numerical re-

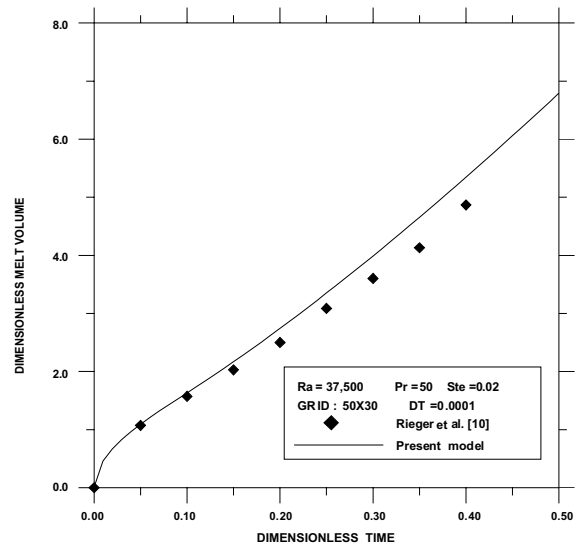


Fig. 15. Comparison of the predicted dimensionless melt volume with the results of Rieger et al. [10] for  $Ra = 37,500$ .

sults were compared with available numerical results due to Prusa and Yao [11,12] and Rieger et al. [10]. The agreement is found to be satisfactory indicating that the proposed model is adequate to represent the physical situation of fusion around a horizontal cylinder in the presence of natural convection in the melt region.

#### Acknowledgements

The authors wish to thank the CAPES for the scholarships and FAPESP for the financial support.

#### References

- [1] H.G. Landau, Heat conduction in a melting solid, *Quart. Appl. Math.* 8 (1) (1950) 81–94.
- [2] J.L. Duda, M.F. Malone, R.H. Notter, J.S. Ventras, Analysis of two-dimensional diffusion-controlled moving boundary problems, *Int. J. Heat Mass Transfer* 18 (7) (1975) 901–910.
- [3] T. Saitoh, Numerical method for multi-dimensional freezing problems in arbitrary domains, *ASME J. Heat Transfer* 100 (1978) 294–299.
- [4] E.M. Sparrow, S. Ramadhyani, S.V. Patankar, Effect of subcooling on cylindrical melting, *ASME J. Heat Transfer* 100 (1978) 395–402.
- [5] R.M. Furzerland, A comparative study of numerical methods for moving boundary problems, *J. Inst. Math. Appl.* 26 (4) (1980) 411–429.
- [6] R. Viswanath, Y. Jaluria, A comparison of different solution methodologies for melting and solidification problems in enclosures, *Numer. Heat Transfer—Part B* 24 (1993) 77–105.



- [7] E.M. Sparrow, S.V. Patankar, S. Ramadhyani, Analysis of melting in the presence of natural convection in the melt region, *ASME J. Heat Transfer* 99 (1977) 520–526.
- [8] L.S. Yao, F.F. Chen, Effects of natural convection in the melted region around a heated horizontal cylinder, *ASME J. Heat Transfer* 102 (1980) 667–672.
- [9] L.S. Yao, W. Cherney, Transient phase-change around a horizontal cylinder, *Int. J. Heat Mass Transfer* 24 (12) (1981) 1971–1981.
- [10] H. Rieger, U. Projahn, H. Beer, Analysis of the heat transport mechanisms during melting around a horizontal circular cylinder, *Int. J. Heat Mass Transfer* 25 (1) (1982) 137–147.
- [11] J. Prusa, L.S. Yao, Melting around a horizontal heated cylinder: Part—I Perturbation and numerical solutions for constant heat flux boundary condition, *ASME J. Heat Transfer* 106 (2) (1984) 376–384.
- [12] J. Prusa, L.S. Yao, Melting around a horizontal heated cylinder: Part—II Numerical solution for isothermal boundary condition, *ASME J. Heat Transfer* 106 (2) (1984) 469–472.
- [13] J. Herrmann, W. Leindenfrost, R. Viskanta, Melting of ice around a horizontal isothermal cylindrical heat source, *Chem. Eng. Commun.* 25 (1984) 63–78.
- [14] C.-J. Ho, S. Chen, Numerical simulation of melting of ice around a horizontal cylinder, *Int. J. Heat Mass Transfer* 29 (9) (1986) 1359–1369.
- [15] E.M. Sparrow, R.R. Schmidt, J.W. Ramsey, Experiments on the role of natural convection in the melting of solids, *ASME J. Heat Transfer* 100 (1978) 11–16.
- [16] N.W. Hale, R. Viskanta, Solid–liquid phase-change heat transfer and interface motion in materials cooled or heated from above or below, *Int. J. Heat Mass Transfer* 23 (3) (1980) 283–291.